

Identifying Origin of Self-Similarity in EcoSim, an Individual-Based Ecosystem Simulation, using Wavelet-based Multifractal Analysis

Abbas Golestani and Robin Gras

Abstract— This paper presents a multifractal analysis of the data generated by the ecosystem simulation, EcoSim. A wavelet-based method has been used for this analysis. Multifractal analysis of EcoSim's results demonstrates self-similarity characteristics in the spatial distribution of individuals as it has been observed in real ecosystems. One important issue for ecologists is to understand where these structures come from. We analyzed different parameters of the simulation to detect which ones cause the multifractal behavior. We showed that the combination of the predation pressure associated with the distribution of food is an important factor for the emergence of multifractal phenomena. These results also prove the capacity of EcoSim to generate data with complex characteristics generally observed in real ecosystem studies.

Index Terms— ecosystem simulation, modeling, multifractal analysis, wavelet transform

I. INTRODUCTION

RECENTLY, researchers have begun to recognize the ecosystem data as a highly nonlinear system [1]. Analysis of time series with high complexity, such as time series resulting from the interaction between individuals' behaviors in ecosystems, requires a nonlinear dynamical approach [2-5]. Dynamic studies of nonlinear systems allow to describe the specification of biological processes [6]. These methods are applicable to signals with a low dimensional deterministic nature. Most of the scientists believe that a chaotic behavior can be observed in many natural systems, such as the weather [7], and natural phenomena have to be considered as chaotic systems [8]. Therefore nonlinear dynamic methods based on the concept of chaos have been used to analyze ecosystem time series [9]. In most of the natural phenomena chaotic and self-similarity properties co-exist [10], [11]. Since the seminal work of Mandelbrot [12], many patterns and processes have proven to be efficiently described by fractals in many fields of the natural sciences. Fractal geometry and their resulting scaling properties have also been suggested as a way to characterize space-time heterogeneity in ecology [13].

Manuscript received July 06, 2012; revised August 06, 2012. This work was supported by the NSERC grant ORGPIN 341854, the CRC grant 950-2-3617 and the CFI grant 203617 and is made possible by the facilities of the Shared Hierarchical Academic Research Computing Network.

Abbas Golestani is with the School of Computer Science, University of Windsor, ON N9B3P4 Canada (e-mail: golesta@uwindsor.ca).

Robin Gras is with the School of Computer Science and Department of Biology, University of Windsor, ON N9B3P4 Canada (e-mail: rgras@uwindsor.ca).

Fractals identify the presence of patterns at multiple scales. Part of the fractals' appeal is that a single statistic can be used to describe potentially complex patterns in natural environments. The use of fractal geometry can be viewed as a tool to be used by landscape ecologists to aid in answering questions relating to scale [14]. Studies have shown that natural phenomena present self-similar property over time [15].

A multifractal system is a generalization of a fractal system in which a single exponent (the fractal dimension) is not enough to describe its dynamics; instead, a continuous spectrum of exponents is needed. Self-similarity is a typical property of fractals. Scale invariance is an exact form of self-similarity where at any magnification, there is a smaller piece of the object that is similar to the whole [2]. Applications of multifractals to ecology still remain anecdotic, limited to forest ecology [16], [17], population dynamics [18], the characterization of species-area relationship, species diversity, and species abundance distribution [19], [20], and the characterization of nutrient, phyto- and zooplankton patchiness [21], [22]. Multifractal analysis techniques allow exploring features of signal distribution that are not considered very often [15]. In this paper, a wavelet-based method has been used for multifractality analysis. The wavelet transform takes advantage of multifractal self-similarities, in order to compute the distribution of their singularities. This singularity spectrum is used to analyze multifractal properties [23].

It has been shown that EcoSim, a large scale evolving predator-prey ecosystem simulation can be used to perform studies in theoretical biology and ecology [24], [25]. It has been shown in [9] that behavior of population in EcoSim is chaotic and in this paper we want to show that multifractal property also exists in spatial distribution of individuals. One of the issues ecologists have to deal with is not only to observe multifractal spectrum for the spatial distribution, but also to explain, from a phenomenological point of view where these structures come from. Because many environmental parameters display self-similarity, the observed biotic patterns could reflect the distribution of some abiotic factors presenting a template upon which individual operate [15], [26]. For this reason we analyzed different parameters of EcoSim such as the pattern of food, the predators' pressure and the raggedness of the environment to detect the factors which can explain multifractal behavior in spatial distribution of individuals.

Because this simulation is a logical description of how a simple ecosystem performs, this analysis can help biologists to better understanding of long-term behavior of ecosystem. We analyzed the spatial distribution of individuals in various simulation experiments: one that used no specific pattern of food in world (EcoSim), experiment that has no predator (EcoSimNoPredator), experiments that used a specific pattern of food (EcoSimCircle, EcoSimStar) and experiments with obstacle cells in the world (EcoSimObstacle1%, EcoSimObstacle10%).

The paper is organized as follows: in next section, we present the EcoSim. Thereafter, we explain the wavelet-based methods for the multifractal analysis. Finally, we present the results of applying multifractal analysis method to the different ecosystem simulation data.

II. SIMULATION

In this section, the main parts of the evolving agent-based predator/prey ecosystem (EcoSim) are briefly introduced. The comprehensive description of this simulation has been proposed by [27]. This simulation is a logical description of how a simple ecosystem performs. In this simulation, complex adaptive agents (or, simply, individuals), each one of them using a Fuzzy Cognitive Map (FCM) as a behavioral model, are either a prey or a predator in a virtual world implemented as a 1000×1000 matrix of cells.

A. Fuzzy Cognitive Maps

FCMs are weighted graphs aiming to represent the causal relationship between concepts and to analyze inference patterns. In EcoSim, the FCM is not only the base for describing and computing the agent behaviors, but also the platform for modeling the evolutionary mechanism and the speciation events as it is coded in the individual's genome. Each individual performs an action during a time step based on its perception of the environment. The FCM (called a map in the simulation) is used to model the agent behaviors (structure of the graph) and to compute the next action of the agent (dynamics of the map). A map contains three kinds of concepts: sensitive, internal, and motor. The activation level of a sensitive concept is computed by a fuzzification of the information coming from the environment (see Fig. 1). The activation level of the motor concept is used to determine what the next action of the agent will be, and a defuzzification of its value can be used to determine the amplitude of the action. Finally, the internal concepts' activation levels correspond to the levels of intensity of the internal states of the agent and affect the computation of the dynamic of the map.

B. Intelligent Agents

Each agent has one FCM and several properties that determine its physical capabilities and its behaviors. The behaviors are determined by the interaction between the FCM and the environment. Each agent possesses its own FCM (coded by its genome, which is subject of the evolutionary process). The FCM contains sensitive concepts

like foeClose, foodClose, energyLow, internal concepts like fear, hunger, curiosity, satisfaction, and motor concepts like evasion, socialization, exploration, breeding. It also contains links and weights representing the mutual influences between these concepts. The FCM of an agent is transmitted to its offspring after being combined with the one of the other parent and after the possible addition of some mutations. The behavioral model of each agent is therefore, unique.

As an example, a very simple map can be defined to model an prey agent perceiving and reacting to its distance from a foe (predator). The closer the foe, the more frightened the agent. Depending on this distance and also on the fear level, the agent will decide whether it will evade or not. The more frightened the agent, the faster the evasion. A FCM corresponding to this example is given in Fig. 1. In this example, there are two sensitive concepts: *foeClose* and *foeFar*, one internal: *fear* and one motor: *evasion*. There are also three influence edges: closeness to a foe excites fear, distance to a foe inhibits fear and fear causes evasion. Activations of the concepts *foeClose* and *foeFar* are computed by fuzzification of the real value of the distance to the foe, and the defuzzification of the activation of *evasion* tells us about the speed of the evasion. In EcoSim, each individual posses its proper map which contains about 30 concepts and hundreds of edges.

In this simulation, a species is a set of individuals associated with the average of the genetic characteristics of its members. The average map of a species is computed based on the FCM matrices of all individuals' members of this species. It is considered that a species splits if the difference between the maps of the two most dissimilar agents in the species is greater than a threshold; the threshold is the same for all species [27], [28].

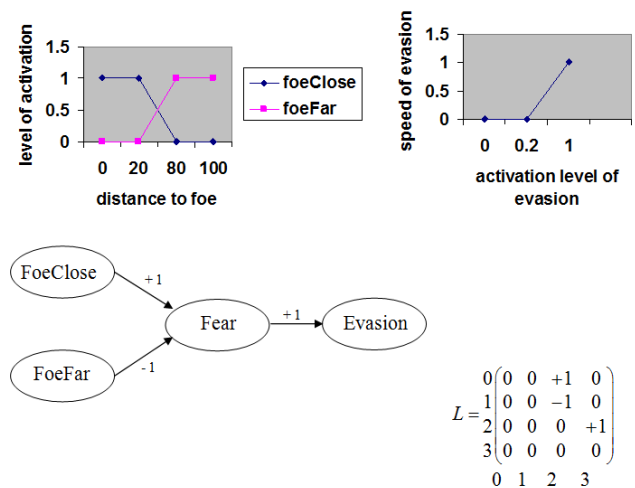


Fig 1. A simple fuzzy cognitive map for detection of foe (predator) and decision to evade with its corresponding matrix with 0 for "Foe close", 1 for "Foe far", 2 for "Fear" and 3 for "Evasion" and the fuzzification and defuzzification functions.

The speciation method consists in applying a 2-means clustering algorithm. With this process an initial species is split into two new species, each one of them containing the agents that are mutually the most similar. At each time step, the values of the states of all the parameters in the model are

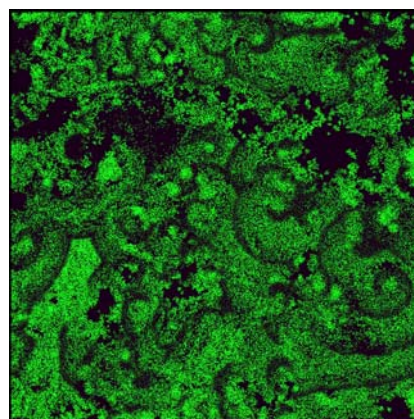
updated. The successive phases of the update process are as follows for each agent: perception of the environment, computation of all concepts of its map, application of their selected action and update of the energy level. Then, there is an update of the lists of agents, species and cells of the world. For each action which requires the agent movement, its speed is proportional to the level of activation of the corresponding action concept.

C. Food Pattern

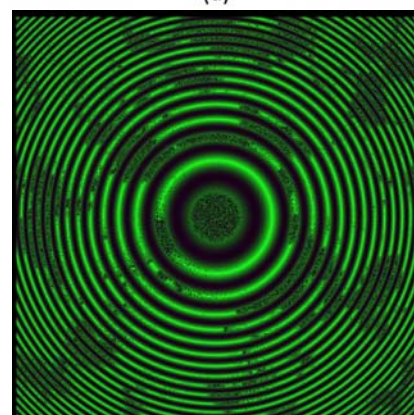
Each cell can contain grass. There is a limit in the amount of grass available in each cell. This allows a competition for resource between individuals to occur. At the initialization time, the number of grass units is uniformly randomly determined for each cell. The number of grass units grows at each time step. The number of grass units in a cell decreases by one when a prey eats. If the prey eats all the grass in one cell the grass cannot grow anymore unless there is still grass in an adjacent cell. This later concept models the mechanism of diffusion of resources through the world changing and renewing the interest of regions of the world (Fig. 2a). We defined two other versions of the simulation based on specific pattern of food distribution. In the first version the food is distributed in concentric circles, we call it EcoSimCircle (see Fig. 2b). The second one, having the distribution shown in Fig. 2 is called EcoSimStar (Fig. 2c).

D. The Raggedness of Environment

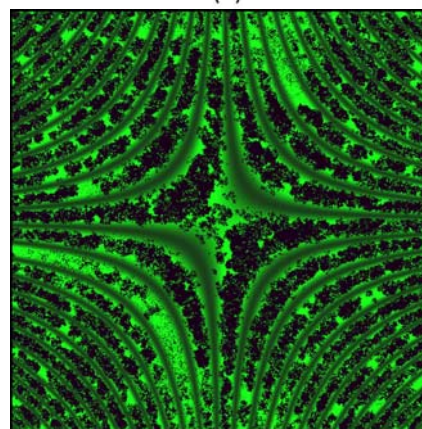
We use also another version of EcoSim simulation to measure effect of the environment's raggedness on population fragmentation and speciation processes [25]. In order to do that small physical obstacles are included that obstruct the movement (dispersal) of agents. Each obstacle covers completely one cell and they also impede the vision of the individuals. The presence of obstacle cells in the world is also expected to disrupt the movement of the agents, change their spatial distribution, and in turn influence dispersal and ultimately the gene flow between populations. Two virtual worlds with various numbers of obstacles are considered: 1% and 10%. For example, in experiment "EcoSimObstacle 10%", ten percent of cells in world are obstacles. The spatial distribution of individuals in this version of simulation has been shown in Fig. 3 (different color for different species). Each execution of the simulation for this analysis produced approximately 16,000 time steps in 23 days. The computed average and standard deviation for the number of prey individuals are 190,000 and 25,000 respectively (for predator 30,000 and 8,000) and the average and standard deviation for the number of prey species are 49 and 10 (for predator 58 and 9).



(a)



(b)



(c)

Fig 2. Distribution of food (grass) after 10000 time steps in (a) EcoSim (b) EcoSimCircle (c) EcoSimStar

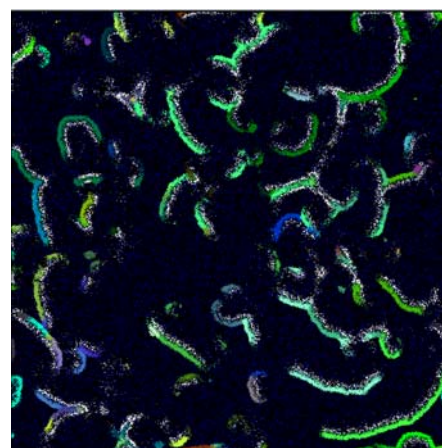


Fig 3. The spatial distribution of individuals in the world with obstacles (EcoSimObstacle10%). The blue dots are obstacle cells.

III. THE CONTINUOUS WAVELET TRANSFORM (CWT) AND WAVELET-BASED MULTIFRACTAL ANALYSIS

Multifractal analysis using the wavelet transform is a powerful tool for detecting self-similarity [29]. The wavelet transform is a convolution product of the data sequence (a function $f(x)$, where x is usually a time or space variable and correspond in this study to time steps,) with the scaled and translated version of the mother wavelet, $\psi(x)$ [29]. The scaling and translation are performed by two parameters; the scale parameter s stretches (or compresses) the mother wavelet to the required resolution, while the translation parameter b shifts the analysing wavelet to the desired location:

$$(Wf)(s, b) = \frac{1}{s} \int_{-\infty}^{+\infty} f(x) \cdot \psi^* \left(\frac{x-b}{s} \right) dx \quad (1)$$

where s, b are real, $s > 0$ for the continuous version (CWT) and ψ^* is the complex conjugate of ψ . The wavelet transform acts as a microscope: it reveals more and more details while going towards smaller scales, i.e. towards smaller s values. The mother wavelet ($\psi(x)$) is generally chosen to be well localized in space (or time) and frequency [30].

Usually, $\psi(x)$ is only required to be of zero mean, but for the particular purpose of multifractal analysis $\psi(x)$ is also required to be orthogonal to some low order polynomials, up to the degree n :

$$\int_{-\infty}^{+\infty} x^m \psi(x) dx = 0, \quad \forall m, \quad 0 \leq m < n \quad (2)$$

Thus, while filtering out the trends, the wavelet transform can reveal the local characteristics of a signal, and more precisely its singularities. (The Hölder exponent can be understood as a global indicator of the local differentiability of a function.) By preserving both scale and location (time, space) information, the CWT is an excellent tool for mapping the changing properties of non-stationary signals.

It can be shown [30] that the wavelet transform can reveal the local characteristics of f at a point x_0 . More precisely, we have the following power law relation:

$$W^{(N)} f(s, x_0) \sim |s|^{h(x_0)} \quad (3)$$

where h is the Hölder exponent (or singularity strength). The symbol “ (N) ”, which appears in the above formula, shows that the wavelet used ($\psi(x)$) is orthogonal to polynomials up to degree n (including n). The scaling parameter (the so-called *Hurst exponent*) estimated when analyzing time series by using “monofractal” techniques is a global measure of self-similarity in a time series, while the singularity strength h can be considered a local version (i.e. it describes “local similarities”) of the *Hurst exponent*. In the case of monofractal signals, which are characterized by the same singularity strength everywhere ($h(x) = ct$), the Hurst exponent equals h . Depending on the value of h , the input series could be long-range correlated ($h > 0.5$), uncorrelated ($h = 0.5$) or anti-correlated ($h < 0.5$).

To characterize the singular behavior of functions, it is sufficient to consider the values and position of the Wavelet Transform Modulus Maxima (WTMM) [31]. The wavelet modulus maxima is a point (s_0, x_0) on the scale-position plane, (s, x) , where $|Wf(s_0, x_0)|$ is locally maximum for x in

the neighborhood of x_0 . These maxima are located along curves in the plane (s, x) . The WTMM representation has been used for defining the partition function based multifractal formalism [32], [33].

Let $\{u_n(s)\}$, where n is an integer, be the position of all local maxima at a fixed scale s . By summing up the q 's power of all these WTMM, we obtain the partition function Z :

$$Z(q, s) = \sum_n |Wf(u_n, s)|^q \quad (4)$$

By varying q in Eq. (4), it is possible to characterize selectively the fluctuations of a time series: positive q 's accentuate the “strong” inhomogeneities of the signal, while negative q 's accentuate the “smoothest” ones. In this work, we have employed a slightly different formula to compute the partition function Z by using the “supremum method”, which prevents divergences from appearing in the calculation of $Z(q, a)$, for $q < 0$ [33].

Often scaling behavior is observed for $Z(q, s)$ and the spectrum $\tau(q)$, which describes how Z scales with s can be defined:

$$Z(q, s) \sim s^{\tau(q)} \quad (5)$$

If the $\tau(q)$ exponents define a straight line, the analyzed signal is a monofractal; otherwise the fractal properties of the signal are inhomogeneous, i.e. they change with location, and the time series is a multifractal. By using the Legendre transformation we can obtain the multifractal spectrum $D(h)$ from $\tau(q)$.

IV. RESULTS OF MULTIFRACTAL ANALYSIS USING WAVELETS-BASED METHOD

It is essential to measure the correlation between the positions of the main biotic factors to gain new insights into the origin of distributions in biological systems. For that reason the effects of two environmental parameters and the effect of predators' pressure on prey's spatial distribution have been examined. The snapshots considered in the analysis correspond to a typical spatial distribution of the individuals, and the same results have been obtained at different time steps. For each experiment, we conducted five independent runs using the same parameters and averaged the results.

A. Predators' pressure

This section is an analysis of the spatial distribution of prey individuals generated by two simulations: EcoSim and EcoSimNoPredator (EcoSim with no predator in the world) in order to investigate the effect of predators' pressure. Multifractal spectra have been calculated for the spatial distribution of prey individuals in both experiments. In both experiments there is an initial uniform random distribution of food. The evolution of the individuals and their interactions then shape the spatial distribution of individuals.

The spatial distribution of individuals for EcoSim and EcoSimNoPredator simulation are shown in Fig. 4 (different color for different species). Contrary to the emerging herd patterns observed in the EcoSim simulation (Fig. 4a), the spatial distribution of individuals in the other simulation

forms simpler patterns, which prey expand in all direction in absence of predators (Fig. 4b).

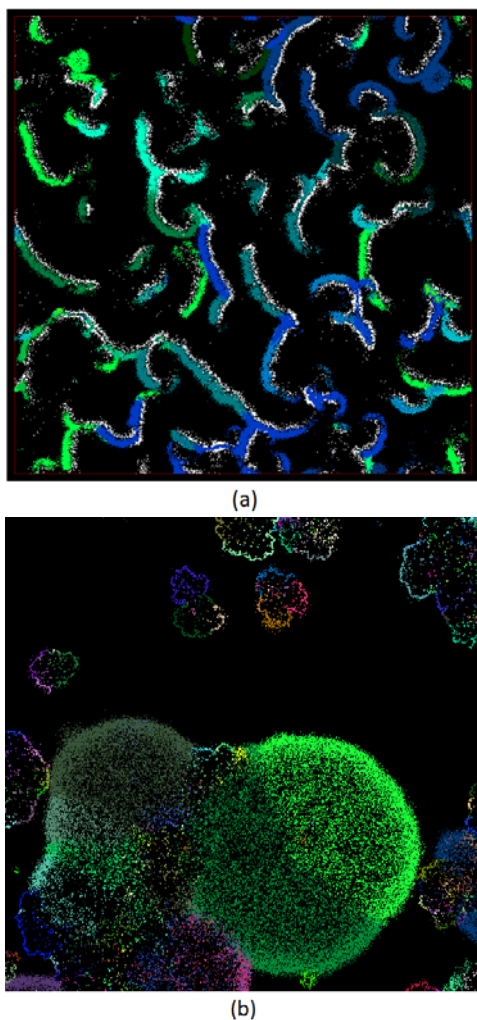


Fig 4. Spatial distribution of individuals in (a) EcoSim (b) EcoSimNoPredator

Fig. 5 shows the *CWT* representation of the prey individuals' spatial distribution in EcoSim. From an intuitive point of view, the wavelet transform shows a “resemblance index” between the signal and the wavelet. If a signal is similar to itself at different scales, then the “resemblance index” or wavelet coefficients also will be similar at different scales. In the coefficients plot (Fig. 5), which shows scale on the vertical axes, this self-similarity generates a characteristic pattern. This is a good demonstration of how well the wavelet transform can reveal the fractal pattern of the behavioral activity at different times and scales.

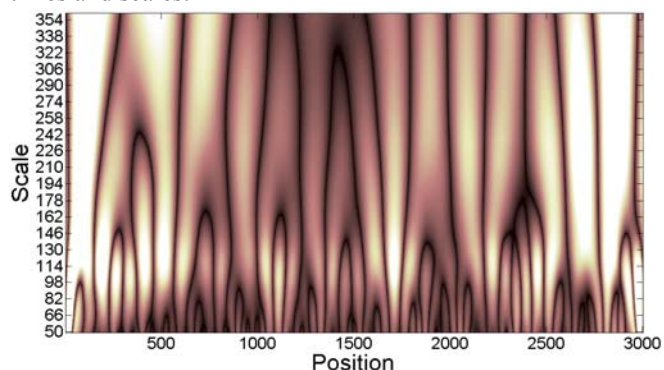


Fig 5. CWT coefficients plot of the spatial distribution of prey individuals

in EcoSim. Scale and position are on the vertical and horizontal axis, respectively.

Fig. 6a displays the “tau spectrum, $\tau(q)$ ”, obtained by using the *WTMM* method, applied to the spatial distribution of prey individuals in the EcoSim experiment. The spectrum is curved, which indicates the multifractal nature of the spatial distribution. We computed the spectrum $D(h)$, represented in Fig. 6b, which clearly confirms the non-uniqueness of the Hölder exponent h , and thus the multifractality of the process.

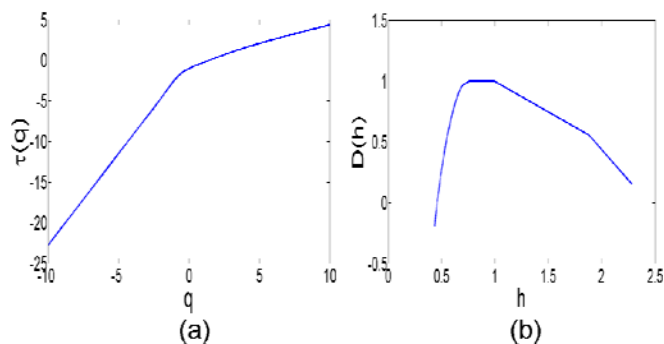


Fig 6. (a) “Tau spectrum” of the spatial distribution of prey individuals in EcoSim (b) Multifractal spectrum of the spatial distribution of prey individuals in EcoSim. By analyzing the spectrum one can assume a multifractal process. Every curve represents an average value obtained from five independent runs.

These results shown that the interaction between individuals over the time and the uniform distribution of food in the world make a complex spatial distribution of prey individuals with multifractal characteristics.

As the food is initially uniformly distributed, it cannot be the leading factor that generates the fractal property. Since this is a prey-predator model, the behaviors of prey and predator have to evolve simultaneously to give them the abilities needed to survive, so the affect of predator is important in this matter. Therefore the multifractal analysis was also applied to the spatial distribution of predators. The results show that the spatial distribution of predators has the same multifractal characteristics as the spatial distribution of prey (data not shown). These results confirm previous results real data, such as the population dynamics of soil microorganisms [34], the swimming behavior of the calanoid copepod *Temora longicornis*, the displacements of male *Daphniopsis australis* and the microphytobenthos biomass distribution [15], that have multifractal properties.

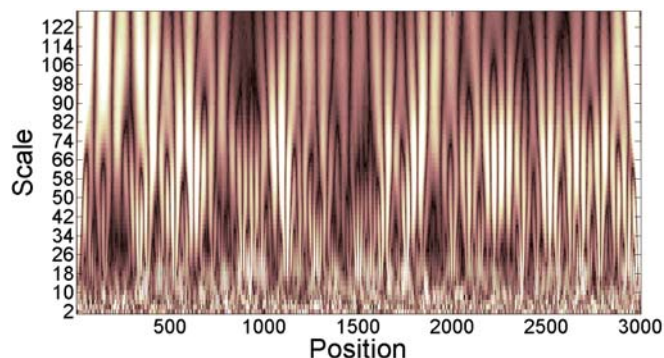


Fig 7. CWT coefficients plot of the spatial distribution of prey individuals in EcoSimNoPredator. Scale and position are on the vertical and horizontal axis, respectively.

The wavelet analysis has been also applied to the spatial distribution of prey individuals in EcoSimNoPredator simulation. The EcoSimNoPredator simulation's parameters are identical, with the same initial parameters and scales and population dynamic in the EcoSim. The only difference is absence of predators in the world. In the coefficients plot (Fig. 7), there is no pattern like the patterns in Fig. 5. Therefore, at least from a visual point of view, it seems that there is no self-similar pattern.

Fig. 8a displays the "tau spectrum, $\tau(q)$ ", obtained by using the WTMM method, for the prey individuals' spatial distribution. The spectrum is not curved, confirming that there is no multifractal property in these patterns. We obtain the spectrum $D(h)$, represented in Fig. 8b, which clearly does not confirm the non-uniqueness of the Hölder exponent h . The figure shows just a straight line which stands for one value thus the multifractality of the spatial distribution can be rejected.

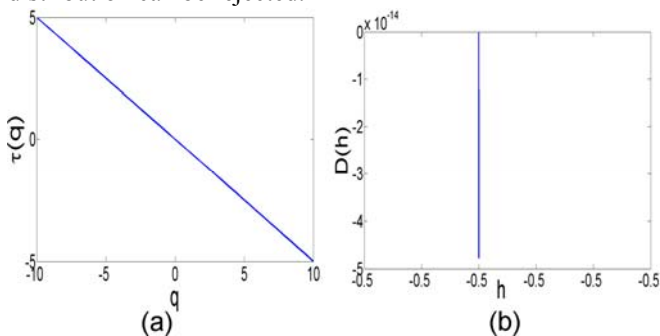


Fig 8. (a) "Tau spectrum" of the spatial distribution of prey individuals in EcoSimNoPredator (b) Multifractal spectrum of the spatial distribution of prey individuals in EcoSimNoPredator. By analyzing the spectrum one can assume a multifractal process. Every curve represents an average value obtained from five independent runs.

This outcome showed that the predators' pressure can lead to a multifractal behavior when there is no limit on mobility of individuals. With equal ease of movement in all directions, predators will be able to push prey in different scales. Individuals distribution forming spiral waves is one property of prey-predator models (like in Fig. 4a). The prey near the wave break have the capacity to escape from the predators sideways. A subpopulation of prey then finds itself in a region relatively free from predators. In this predator-free zone, prey start expanding intensively and form a circular expanding region. The whole pressure process and spiral formation will be applied to this subpopulation of prey and predators again leading to the formation of a second scale. This process repeats over and over and this is a common property of self-similar processes [35]. Because there are consecutive interactions between prey and predators during time, the same pattern repeats over and over and then self-similarity emerges in spatial distribution of individuals.

Indeed, prey distribution and food distribution are very important for predators because food availability changes depending on the fractal dimension. Non-multifractal behavior indicates a smooth and predictable distribution of particles gathered in small numbers of patches, while multifractal behavior indicates rough, fragmented, space-filling and less predictable distributions. When a predator has no remote detection ability (which is our case because predators don't have long range vision), prey distributions

with multifractal behavior could be efficient for predators, because available food quantity become proportional to the searched volume as multifractal behavior increases [15].

B. Various Food Pattern

This section is an analysis of the simulation's spatial distribution of prey individuals generated by two simulations: EcoSimCircle (EcoSim with circle pattern of food) and EcoSimStar (EcoSim with star pattern of food) in order to investigate the effect of food pattern. Multifractal spectra have been calculated for the spatial distribution of prey individuals in all experiments. In EcoSimCircle and EcoSimStar, the spatial distribution of food is kept fixed during the whole simulation.

The spatial distribution of individuals for EcoSimCircle and EcoSimStar simulation are shown in Fig. 9. Contrary to the emerging herd patterns observed in the EcoSim simulation (Fig. 4a), the spatial distribution of individuals in the these two simulations followed the circle and star food distribution respectively (Fig. 9a, 9b). For space consideration, we do not present the graphs of the multifractal analysis as they are almost identical to the ones already presented.

The wavelet analysis has been applied to the spatial distribution of prey individuals in EcoSimCircle simulation. The EcoSimCircle simulation's parameters are kept the same, with the same initial parameters and scales and population dynamic in the EcoSim. The only difference is the fixed distribution of food in the world.

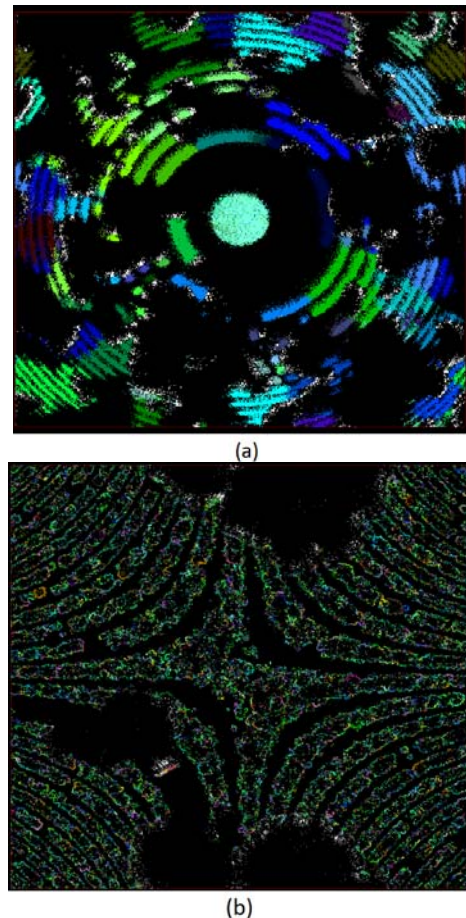


Fig 9. Spatial distribution of individuals in (a) EcoSimCircle (b) EcoSimStar

In the coefficients plot, there is no self-similar patterns like the patterns in Fig. 5. Multifractal spectrum have been calculated for the spatial distribution of prey individuals. The “*tau spectrum, $\tau(q)$* ” and the spectrum $D(h)$ (like Fig. 8), clearly demonstrate that there is no multifractal behavior in the spatial distribution of prey (results not shown). The multifractal analysis was also applied to the spatial distribution of predators in this experiment. The result shows there is no multifractal characteristic in spatial distribution of predators. The same wavelet-based analysis has been applied to EcoSimStar and the same results have been obtained: no multifractal pattern for grass and for spatial distribution of prey and predators. When the distribution of food in the world becomes fixed, the multifractal phenomenon vanished. Therefore, as long as there is specific fixed pattern of food in the world it seems that the complex multifractal phenomenon doesn't show up for spatial distribution of individuals. The dynamic distribution of food is needed for complex patterns to emerge as it strongly affects the spatial distribution of the prey that need this food to survive.

C. Various Levels of Environment's Raggedness

We are also interested in studying whether various levels of raggedness in the world, as it also has impact on the movement of the individuals, can affect the fractal properties observed. We use two new simulation experiments with various numbers of obstacles: 1 and 10 per cent, EcoSimObstacle(1%) and EcoSimObstacle(10%). The raggedness of the world increases when the number of obstacle cells raises. Multifractal spectrum have been calculated for the spatial distribution of individuals in all these experiments and compared them with results of EcoSim.

In EcoSim, there is no obstacle cells in the world and the results of this simulation has been shown in previous section which shows existence of multifractal behavior in individuals' spatial distribution. We measured the *CWT* representation of the individuals' spatial distribution for EcoSimObstacle(1%) and EcoSimObstacle(10%). The coefficients plot (like Fig. 5), the “*tau spectrum, $\tau(q)$* ” and the spectrum $D(h)$ (like Fig. 6), clearly demonstrate the multifractality of the process.

In these two experiments, with different level of raggedness, a multifractal behavior also emerged. We can conclude that this parameter doesn't play a major role in multifractal behavior of spatial distribution. Regardless of the level of raggedness, individuals finally find their way to adopt and form the complex pattern.

V. CONCLUSION

The purpose of this paper is to analyze the multifractal behaviors of individuals' spatial distribution that are produced by the ecosystem simulation (EcoSim). Understanding of the origin of individuals patchiness is an important issue. It is stressed here that the knowledge of the multifractal distributions of relevant parameters such as food concentration, spatial distribution of prey and predators and density of obstacles could be the first step to infer their phenomenological links. We applied our analysis

to different kinds of simulations: the ecosystem simulation with fixed specific pattern of food in the world, the world without predators' pressure and the world with several amounts of obstacles and then we compared the results with the ones obtained with the simulation without constraints.

We used a wavelet-based method for this analysis. It showed that the behavior of the individuals without any constraints, or restricted by a limited amount of obstacles with predators' pressure can lead to the multifractal phenomena as the ones observed in real ecosystems. It is also another important confirmation of the capacity of EcoSim to model complex and realistic large scale systems. On the contrary, we have shown that when the food distribution is fixed, which strongly reduces the possibility of movement of the prey, the multifractal pattern disappears. It seems that it is the complex interaction between the predation pressure, the eating behavior of the prey and the diffusion of food that conducts to the apparition of the multifractal phenomenon.

There are a number of possible extensions of this study. We will be interested to analyze other versions of the current simulation or even other different simulations. We will be also interested to compare more into detail the correspondence between the patterns observed in EcoSim with the ones coming from real data. Finally, we will be interested to see if different kinds of ecosystems can be characterized by different multifractal properties. We will be able to use EcoSim to investigate different hypotheses and to see what properties of the system have an influence on the multifractal patterns.

REFERENCES

- [1] H. Kantz and T. Schreiber, *Nonlinear Time Series Analysis*, vol. 7, no. 3. Cambridge University Press, 1997, p. 304.
- [2] C. J. Stam, “Nonlinear dynamical analysis of EEG and MEG: review of an emerging field,” *Clinical Neurophysiology*, vol. 116, no. 10, pp. 2266-2301, 2005.
- [3] M. E. Brandt, A. Ademoglu, and W. S. Pritchard, “Nonlinear Prediction And Complexity Of Alpha Eeg Activity,” *International Journal of Bifurcation and Chaos*, vol. 10, no. 1, pp. 123-133, 2000.
- [4] W. Kinsner, “A unified approach to fractal dimensions,” *Fourth IEEE Conference on Cognitive Informatics 2005 ICCI 2005*, vol. 1, no. December, pp. 58-72, 2005.
- [5] A. H. Meghdadi, W. Kinsner, and R. Fazel-Rezai, “Characterization of healthy and epileptic brain EEG signals by monofractal and multifractal analysis,” *2008 Canadian Conference on Electrical and Computer Engineering*, pp. 001407-001412, May 2008.
- [6] A. Golestani, A. Ashouri, K. Ahmadian, M. Jahed-Motlagh, and M. Doostari, “Irregularity Analysis of Iris patterns,” *IPCV08*, 2008.
- [7] R. Sneyers, “Climate Chaotic Instability: Statistical Determination And,” *Environmetrics*, vol. 8, no. February, pp. 517-532, 1997.
- [8] L. Romanelli, M. A. Figliola, and F. A. Hirsch, “Deterministic chaos and natural phenomena,” *Journal of statistical physics*, vol. 53, no. 3, pp. 991-994, 1988.
- [9] A. Golestani and R. Gras, “Regularity analysis of an individual-based ecosystem simulation,” *Chaos*, vol. 20, no. 4, p. 3120, 2010.
- [10] A. Bershadskii, “Some universal properties of multifractal chaos at nuclear giant resonance,” *Phys.Rev.C*, vol. 59, pp. 3469-3472, 1999.
- [11] R. V. Sole and S. C. Manrubia, “Self-similarity in rain forests: Evidence for a critical state,” *Physical Review-Section E-Statistical Physics Plasma Fluids Related Interdiscipl Topics*, vol. 51, no. 6, pp. 6250-6253, 1995.
- [12] B. B. Mandelbrot, “Self-affine fractal sets, I: the basic fractal dimensions,” in *Fractals in physics*, 1986, vol. 1, p. 3.
- [13] M. G. Turner and R. H. Gardner, *Quantitative methods in landscape ecology: the analysis and interpretation of landscape heterogeneity*, vol. 82. Springer Verlag, 1991.

- [14] B. T. Milne, "Applications of fractal geometry in wildlife biology," in *Wildlife and Landscape Ecology: Effects of Pattern on Scale*, J. A. Bissonette, Ed. New York: Springer and Verlag, 1997, pp. 32-69.
- [15] L. Seuront, *Fractals and multifractals in ecology and aquatic science*. CRC Press, 2010.
- [16] I. Scheuring and R. H. Riedi, "Application of multifractals to the analysis of vegetation pattern," *Journal of Vegetation Science*, vol. 5, no. 4, pp. 489-496, 1994.
- [17] J. B. Drake and J. F. Weishampel, "Multifractal analysis of canopy height measures in a longleaf pine savanna," *Forest Ecology and Management*, vol. 128, no. 1-2, pp. 121-127, 2000.
- [18] J. Ozik, B. R. Hunt, and E. Ott, "Formation of multifractal population patterns from reproductive growth and local resettlement," *Physical Review E*, vol. 72, no. 4, p. 46213, 2005.
- [19] C. Ricotta, "From theoretical ecology to statistical physics and back: self-similar landscape metrics as a synthesis of ecological diversity and geometrical complexity," *Ecological Modelling*, vol. 125, no. 2-3, pp. 245-253, 2000.
- [20] L. Borda-de-Água, S. P. Hubbell, and M. McAllister, "Species-area curves, diversity indices, and species abundance distributions: a multifractal analysis," *The American Naturalist*, vol. 159, no. 2, pp. 138-155, 2002.
- [21] M. Pascual, F. A. Ascoti, and H. Caswell, "Intermittency in the plankton: a multifractal analysis of zooplankton biomass variability," *Journal of plankton research*, vol. 17, no. 6, p. 1209, 1995.
- [22] L. Seuront and N. Spilmont, "Self-organized criticality in intertidal microphytobenthos patch patterns," *Physica A: statistical mechanics and its applications*, vol. 313, no. 3, pp. 513-539, 2002.
- [23] S. G. Mallat, *A wavelet tour of signal processing*. Academic Pr, 1999.
- [24] D. Devaurs, and R. Gras, "Species abundance patterns in an ecosystem simulation studied through Fisher's logseries," *Simul. Model. Pract. Theory* 18, pp 100-123, 2010.
- [25] A. Golestani, R. Gras, and M. Cristescu, "Speciation with gene flow in a heterogeneous virtual world: can physical obstacles accelerate speciation?," *Proceedings of the Royal Society B: Biological Sciences*, vol. 279 no. 1740, 2012, pp 3055-3064, 2012.
- [26] J. M. G. Vilar, R. V. Solé, and J. M. Rubi, "On the origin of plankton patchiness," *Physica A: Statistical Mechanics and its Applications*, vol. 317, no. 1, pp. 239-246, 2003.
- [27] R. Gras, D. Devaurs, A. Wozniak, and A. Aspinall, "An individual-based evolving predator-prey ecosystem simulation using a fuzzy cognitive map as the behavior model," *Artificial life*, vol. 15, no. 4, pp. 423-463, 2009.
- [28] A. Aspinall and R. Gras, "K-means clustering as a speciation mechanism within an individual-based evolving predator-prey ecosystem simulation," *Active Media Technology*, pp. 318-329, 2010.
- [29] P. S. Addison, *The illustrated wavelet transform handbook: introductory theory and applications in science, engineering, medicine and finance*. Taylor & Francis, 2002.
- [30] B. Enescu, K. Ito, and Z. R. Struzik, "Wavelet-Based Multifractal Analysis of real and simulated time series of earthquakes," *Annuals of Disas. Prev. Res. Inst., Kyoto Univ*, no. 47, 2004.
- [31] S. Mallat and W. L. Hwang, "Singularity detection and processing with wavelets," *Information Theory, IEEE Transactions on*, vol. 38, no. 2, pp. 617-643, 1992.
- [32] J.F. Muzy, E. Bacry, and A. Arneodo, "The multifractal formalism revisited with wavelets," *International Journal of Bifurcation and Chaos in Applied Sciences and Engineering*, vol. 4, no. 2, pp. 245-302, 1994.
- [33] A. Arneodo, E. Bacry, and J. F. Muzy, "The thermodynamics of fractals revisited with wavelets," *Physica A: Statistical Mechanics and its Applications*, vol. 213, no. 1, pp. 232-275, 1995.
- [34] J. W. Crawford, K. Ritz, and I. M. Young, "Quantification of fungal morphology, gaseous transport and microbial dynamics in soil: an integrated framework utilising fractal geometry," *Geoderma*, vol. 56, no. 1-4, pp. 157-172, 1993.
- [35] V. N. Biktashev, J. Brindley, a V. Holden, and M. a Tsyganov, "Pursuit-evasion predator-prey waves in two spatial dimensions.," *Chaos (Woodbury, N.Y.)*, vol. 14, no. 4, pp. 988-94, Dec. 2004.